Statistics of quantum transport in metal nanowires with surface disorder

Jérôme Bürki[1], Charles A. Stafford[2]
[1] Lyman Lab of Physics, Harvard University, Cambridge MA 02138, USA

[2] Department of Physics, University of Arizona, 1118 E. 4th St., Tucson AZ 85721, USA

Experimental conductance histograms built from several thousand successive breakings of sodium nanowires [1,2] exhibit peaks up to rather high conductance values ($\sim 100 \times 2e^2/h$). In this paper, we present results from a disordered free-electron model of a metallic nanowire, which was previously successful in describing both conductance histograms and shot noise measurements in gold nanocontacts with much lower conductances.[3] We find in particular that, with a modification of the model of disorder, the conductance histogram can be understood as an interplay of conductance quantization and disorder for low conductances ($G \lesssim 10 \times 2e^2/h$), while peaks corresponding to higher conductance are actually a combination of several "quantized conductance peaks". We also predict a saturation of the shot noise at high conductance to about 1/10 of its classical value $2e\bar{I}$.

1 Introduction

Recent experiments by Yanson *et al.* [1,2] measuring conductance histograms for sodium nanocontacts have revealed the persistance of well-defined conductance peaks up to rather high conductance values, of order $100G_0$, where $G_0 = 2e^2/h$ is the quantum of conductance. A semi-classical calculation of Kassubek *et al.* [4] provided a description of the histograms in terms of the stability of nanowires of certain radii, but the shift of the experimental peaks with respect to quantized conductance values makes it difficult to identify a peak with a particular quantized conductance. We therefore solve in this paper a free-electron model [5] of a metallic nanowire that includes disorder [3] and allows for a more quantitative identification of the peaks, as well as the calculation of other quantities such as shot noise.

The sequence of conductance peaks observed [1,2] at low temperature ($1, 3, 5, 6, \ldots \times G_0$) is suggestive of cylindrical symmetry. We therefore use a three-dimensional model of a cylindrical wire with a constriction, presented in section 2. The extension of the recursive Green's function numerical method [3] to three-dimensional contacts is discussed in section 3. Finally, the results are presented and discussed in section 4.

2 Model

As in previous papers,[3,5] we use a free-electron model of a metallic nanowire. The nanowire is taken to be an infinite cylinder of radius R with a finite deformable part representing the contact, defined by the function $r(z) = R_{min} + (R - R_{min}) \left[3u^2 - 3u^4 + u^6\right]_{u=2z/L}$, where R_{min} is determined at each step of the elongation L such that the volume of the contact is kept constant. Independent electrons are confined within the wire by hard-wall boundary conditions and the Fermi energy of the electron gas is taken to be the bulk sodium Fermi energy, namely $\varepsilon_F = 3.23eV$. All calculation are made at zero temperature.

The bulk model of disorder used previously to model gold nanocontacts [3] is problematic for sodium because of the larger size [1,2] of the contacts: A disorder resistance of a few hundred Ohms is necessary to shift the lower conductance peaks back onto quantized values, corresponding to a conductance of less than $100G_0$. If the disorder resistance is to be constant during elongation of the contact, which is the case with bulk disorder, it would be impossible to measure a conductance larger than this value, which is clearly not the case.[1] We therefore need a model of disorder whose resistance decreases with increasing conductance of the contact.

The material used in experiments being of very high purity, the main source of backscattering is likely to be surface roughness [6] or surface defects. We therefore introduce the following model of surface disorder: (i) As previously,[3] we use δ-function impurities of fixed strength W and random positions; (ii) The initial positions of the impurities are restricted to a length L_{dis} of the conductor that includes the constriction, and within a distance d of the surface of the wire (i.e. $R - d \leqslant r \leqslant R$, r being the radial coordinate of the impurity); (iii) During elongation of the contact, the distance of the impurity to the surface is kept constant, while its longitudinal position is changed such that the linear density of impurities is constant along the wire.

With this model, the resistance due to impurities will increase as the minimal cross-section area decreases. The thickness d of the disordered shell is chosen on physical grounds to be essentially one atomic layer, or $k_F d = 3$. We want to emphasize that this surface disorder model is likely to be a better model for gold as well, but all conductance histograms published for gold [7] were restricted to conductances lower than $10G_0$, in which regime both models give similar results.

3 Method

In principle, the recursive Green's function method used in our earlier paper [3] can be extended without further complication to a three-dimensional model such as considered in this work. In practice, however, one would need a very fine discretization of space in order to reproduce the correct degeneracies of the transverse energy levels, making the computation intractable, especially for the larger contacts we want to consider. Instead, we discretize only the longitudinal coordinate z after the change of coordinates that brings the constriction back to a cylinder, and use a basis of transverse eigenstates of the "free" problem (i.e. without a constriction or disorder) to get a matrix representation of the Hamiltonian of a slice. In order to have a finite matrix, we introduce an energy cutoff, which is chosen such that the number of states considered is of the order of twice the number of open channels. Except for this change of basis and the use of a three-dimensional model, the method is a straightforward generalization of our previous work.[3] Once the transmission matrix $t(\varepsilon_F)$ at the Fermi energy has been obtained from the Green's function,[3] the conductance G and shot noise S_I at zero temperature are computed using the Landauer-type formulae

$$G = \frac{2e^2}{h}\mathrm{Tr}\left(t^\dagger t\right), \qquad S_I = 2e\bar{I}\frac{\mathrm{Tr}\left[t^\dagger t\left(1 - t^\dagger t\right)\right]}{\mathrm{Tr}\left(t^\dagger t\right)}. \tag{1}$$

In order to generate a histogram of conductance, we compute the conductance as a function of elongation for a given configuration of disorder, divide the conductance axis in intervals of size $\Delta G = 0.1G_0$ and count the number of points in each interval. We repeat this for 300 configurations of disorder, averaging at the same time on the geometry of the contact by using different initial lengths L_0 for the constriction ($5 \leqslant k_F L_0 \leqslant 25$). We then smoothen the histogram by taking an average over three bins with relative weights $1, 2, 1$, similarly to what is done in the experiments.[1] We can also resolve individual "quantized" conductance peaks by restricting the elongation to intervals corresponding to a fixed number of open channels of the clean adiabatic wire. As to the shot noise, we average its value at a given conductance, using the same set of data as for the histogram.

4 Results

4.1 Conductance histogram

Following the procedure described above, we generated the histogram of Fig. 1(a). The first two peaks, near G_0 and $3G_0$, can be thought of as individual quantized conductance peaks, broadened and shifted downward slightly by disorder. However, the third peak is a mixture of $5G_0$ and $6G_0$, and higher peaks are typically even more complicated admixtures. In Fig. 1(b), the peak near $28G_0$ is shown, along with its decomposition in terms of individual quantized components; one sees that it is actually composed of many individual peaks. The peaks in the conductance histogram are thus generically not ascribable to individual quantized conductance channels, but rather represent a gross shell structure.[1,2] One notes that the agreement with the experimental results of Yanson *et al.*[1,2] is reasonable for conductances lower than $30G_0$, except for the one peak around $7G_0$, which seems to be out of place, and which will be discussed later. For larger conductance, the peaks start to be out of phase with the experimental peaks, which might have several causes: First of all, the disorder present in the experimental nanowires might be stronger or weaker than that in our model. Secondly, our calculation is made at zero

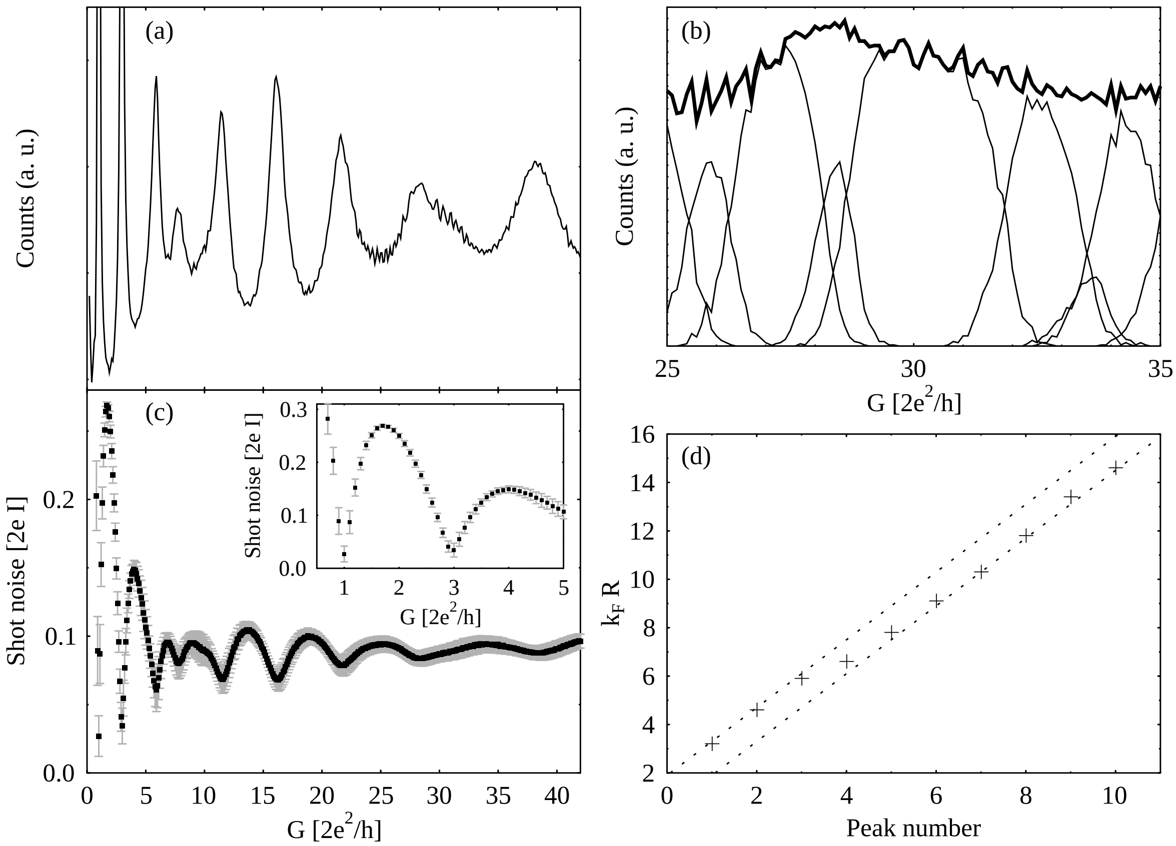

Figure 1: (a) Conductance histogram built from 300 disorder configurations. (b) Blowup of the eighth peak of the histogram (thick line). The thiner lines represent contributions to the histogram from individual "quantized" conductance peaks. (c) Average shot noise of the contact (squares) together with the standard deviation (bars) as a function of the conductance of the contact; the inset blows up the graph at small conductances. (d) Relation between the radius of the wire and the peak number (crosses); the dotted lines are a guide to the eye.

temperature, while the experiment is made around $90K$, where surface diffusion of atoms allows the contact to find more stable configurations, so that those peaks might reflect the stability of the contact, rather than quantum transport effects.

Coming back to the peak near $7G_0$, the discrepancy of its position and its relative weakness suggests that it might actually disappear if a larger amount of disorder was used. In that case, the higher conductance peaks would be shifted further downward, and would presumably correspond to lower experimental peaks. This hypothesis is supported by Fig. 1(d), which shows the radius of the wire, as obtained from the Sharvin formula $G_s = (k_F R/2)^2 (1 - 2/k_F R)$, as a function of the peak number. As is suggested by the two dotted lines, corresponding to a shift of the peak number by one, the linear relation between the radius and the peak number would be better if the fourth peak, which is the peak in question, were removed. The hypothesis of stronger disorder, currently under investigation, seems promising.

4.2 Shot noise

The shot noise, computed as described in Sec. 3, is shown in Fig. 1(c). It shows a strong suppression at low quantized-conductance values and weaker minima corresponding to higher peaks in the conductance histogram, as could be expected from our previous results on gold nanocontacts.[3] At larger conductance values, we observe a saturation of the shot noise at about 1/10 of the classical value $2e\bar{I}$, in contrast to a random-matrix prediction by Beenakker and Melsen [8] of a suppression factor of 1/3 in a disordered nanowire. Part of this discrepancy may come from the difference in disorder (surface versus bulk), but even our results for gold, which used a model much more similar to the one of Ref. [8], showed a saturation value that was about one half of the random-matrix prediction. The reason for this discrepancy is not fully understood, but it may indicate that tunneling through the nanocontact, which is neglected in the model of Ref. [8], plays an essential role in the shot noise in the saturation region, just as it does in the ballistic region at small conductance.

5 Conclusions

We have presented a model of surface disorder in a free-electron nanowire whose numerical solution, using a variation of the Green's function technique presented in our previous paper,[3] helps understand conductance histograms obtained experimentally for sodium nanowires, and provides a prediction for what the shot noise of such wires should look like. Our results show a discrepancy for the saturation value of the shot noise compared to random matrix theory [8] that is so far not understood.

Acknowledgments

JB was supported by a fellowship of the Swiss National Science Foundation. CAS was supported by NSF Grant DMR0072703.

References

1. A. I. Yanson, I. K. Yanson, and Jan M. van Ruitenbeek, *Nature* **400**, 144 (1999).
2. A. I. Yanson, I. K. Yanson, and J. M. van Ruitenbeek, *Phys. Rev. Lett.* **84**, 5832 (2000).
3. J. Bürki, C. A. Stafford, X. Zotos, and D. Baeriswyl, *Phys. Rev. B* **60**, 5000 (1999); J. Bürki and C. A. Stafford, *Phys. Rev. Lett.* **83**, 3342 (1999).
4. F. Kassubek, C. A. Stafford, H. Grabert, and R. E. Goldstein, *Nonlinearity* **14**, 167 (2001).
5. C. A. Stafford, D. Baeriswyl, and J. Bürki, *Phys. Rev. Lett.* **79**, 2863 (1997).
6. A. M. Bratkovsky and S. N. Rashkeev, Phys. Rev. B **53**, 13074 (1996).
7. J. L. Costa-Krämer, N. García, and H. Olin, *Phys. Rev. B* **55**, 12910 (1997).
8. C. W. J. Beenakker and J. A. Melsen, *Phys. Rev. B* **50**, 2450 (1994).